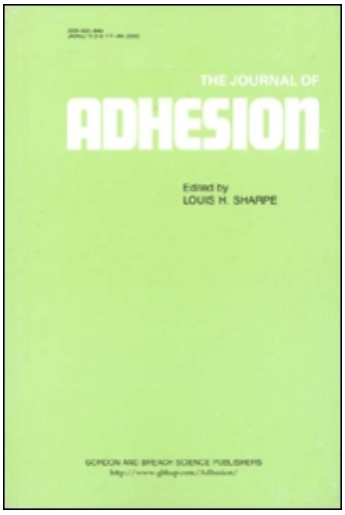

The Journal of Adhesion
Publication details, including instructions for authors and subscription information:
http://www.informaworld.com/smpp/title~content=t713453635

THE FORMATION OF DEPOSITS ON POLYMER SURFACES IN PAPER MACHINE WET END

Timo Kallio[a]; Juha Kekkonen[a]; Per Stenius[a]
[a] Laboratory of Forest Products Technology, Espoo, Finland

Online publication date: 10 August 2010

To cite this Article Kallio, Timo , Kekkonen, Juha and Stenius, Per(2004) 'THE FORMATION OF DEPOSITS ON POLYMER SURFACES IN PAPER MACHINE WET END', The Journal of Adhesion, 80: 10, 933 — 969
To link to this Article: DOI: 10.1080/00218460490508742
URL: http://dx.doi.org/10.1080/00218460490508742

The Journal of Adhesion, 80: 933–969, 2004

ISSN: 0021-8464 print/1545-5823 online
DOI: 10.1080/00218460490508742

Taylor & Francis
Taylor & Francis Group

THE FORMATION OF DEPOSITS ON POLYMER SURFACES IN PAPER MACHINE WET END

Timo Kallio
Juha Kekkonen
Per Stenius
Helsinki University of Technology, Laboratory of Forest Products Technology, Espoo, Finland

Fouling of a negatively charged polyurethane surface by substances typical of those occurring in the wet end of paper machines was studied by QCM-D and AFM. The aim was to evaluate the influence of surface forces, adsorption kinetics, viscoelasticity, and morphology of the adsorbed layers on the fouling process, which is discussed in terms of three steps: (1) contacting of deposits with the surface, (2) adherence of the deposits to the surface, and (3) ability of the adsorbed layer to collect further deposits. Substances studied were pitch emulsions, latex, AKD, kaolin and talc dispersions, cationic starch, and other soluble polymers. pH was 5.5–7. Adsorption tendencies depended, as predicted by the DLVO theory, on the ionic strength and valence of simple ions. Kaolin or polystyrene latex adsorbed only above critical salt concentrations. Strongly coagulated pitch emulsions (large aggregate size) adsorbed to a lesser degree than weakly coagulated emulsions (smaller aggregate size), apparently due to the slower diffusion rate of the larger aggregates.

Received 3 December 2003; in final form 22 June 2004.

The XPS measurements were performed by Joseph Cambell, and the XPS results were interpreted by Leena-Sisko Johansson, Ph.D. at the Center for Chemical Analysis, Helsinki University of Technology. Part of the QCM-D and the light-scattering measurements were done by Ms. Anna-Leena Anttila and Ms. My Linh Ly. Part of the zeta potentials were measured by Juha Lindfors at Metso Paper Oyj, Rautpohja, Finland. Monika Österberg helped with the AFM measurements. Their assistance is gratefully acknowledged. Mikael Danielsson, Juhani Vestola and Leena-Sisko Johansson are thanked for fruitful discussions. Financial support for this work was obtained from Metso Oyj, Rautpohja, Finland and the National Technology Agency of Finland (TEKES).

One of a collection of papers honoring A. W. Neumann, the recipient in February 2004 of *The Adhesion Society Award for Excellence in Adhesion Science, Sponsored by 3M*.

Address correspondence to Timo Kallio, Helsinki University of Technology, Department of Forest Products Technology, P.O. Box 6300, Vuorimiehentie 1, Espoo, FIN-02015 HUT, Finland. E-mail: Timo.Kalio@hut.fi

Current address of Juha Kekkonen is: J. M. Huber Finland Oy, Telakkatie 5, FIN-49460 Hamina, Finland.

Keywords: Fouling; Polyurethane; QCM-D; Quartz crystal microbalance with dissipation monitoring; AFM; Paper machine

INTRODUCTION

Polymeric materials are widely used in the wet end of paper machines. The fouling of polymer surfaces may impair web release [1], decrease paper quality [2], weaken dewatering, and shorten the lifetime of equipment [3]. Although this type of fouling has been studied previously [4–6], the basic surface chemical mechanisms that induce the fouling of polymer surfaces are still not very well known. This article focuses on surface forces and the fouling mechanisms of polyurethane and polyamide. Polyamide is used in press felts [7] and forming fabrics [3]. Polyurethane is used, *e.g.*, as a cover material in press rolls and in shoe press belts [1, 8].

The Growth Mechanisms of Detrimental Deposits

It is useful to divide the process by which detrimental deposits are formed in paper machines into three steps.

The first step is that fouling material is brought into contact with the surface. This may take place through adsorption, collision, sedimentation, phase separation, release of materials from the paper web, or partial drying of aqueous films. In most cases, fouling deposits are formed from dissolved and colloidal substances (DCS) in the process water with dimensions of typically less than micrometers [9]. On the grounds of theoretical calculations presented by Van de Ven and Mason [10], it can be concluded that under the hydrodynamic conditions typical to paper machines such particles do not collide with surfaces through the action of inertial forces only. The most important transport mechanism is diffusion into a range in which attachment to the surface is induced by surface forces. Stagnant points or domains where flow is low and the hydrodynamic forces are weakened should be particularly susceptible to adsorption.

Substances may also be transferred from the paper web to equipment surfaces. The mechanisms involved are poorly studied, and literature reports are mainly limited to some investigations of the transfer of alkyl ketene dimer (AKD) waxes used for sizing [11].

Some surfaces in paper machines, *e.g.*, in rolls in the press section, are intermittently wet and half-dry. This is of importance to fouling,

because the shrinking water film and capillary forces may lead to entanglement of material on the drying surface.

The second step is the adherence of the deposits to the surface. Mechanical and hydrodynamic forces can often remove weakly adhered deposits. Well-adhered deposits are more difficult to detach and potentially more harmful. The strength of adhesion depends on the contact area and the strength of physical interactions or even chemical bonds between the deposits and the surface. It can be argued that most surfaces in paper machines are initially hydrophilic, so preferential bonding of water should substantially weaken acid–base interactions between surface and deposit. Formation of covalent bonds in paper machine environments is likely to be limited to very special cases. Therefore, it can be assumed that predominant factors that control adhesion in the wet end are van der Waals interactions, double layer interactions, ionic bonds, and the contact area between the adhering substance and the surface.

The contact area of rigid particles is often small and hence the total interaction energy with the surface is low. However, many of the materials that form deposits in paper machines, such as pitch, AKD and ASA (Alkylene Succinic Anhydride) waxes, and starch-surfactant complexes, are viscoelastic and thus may be able to spread slowly on the surface and create a large contact area. Liquid contaminants should be easily carried away by hydrodynamic or mechanical forces.

The time that the deposit remains in contact with the surface is also essential. In many cases, prolonged contact times increase adhesion [12].

The third step is the further accumulation of the deposits on the surface. If this does not occur, a fouling layer may remain so thin that it is not necessarily troublesome. A thin adsorbed layer may even spontaneously stop further formation of deposits (*e.g.*, adsorbed polymers may give rise to steric repulsion). Obviously, the surface charge and surface energy of adsorbed material will have an influence on the behaviour of additional potentially fouling substances. Strongly hydrophobic deposits should be able to collect additional hydrophobic material due to long-range hydrophobic attraction [13].

In summary, some substances adsorb but do not stay on the surface due to low adhesion: some adsorb and adhere well, but do not collect further deposits, in which case the growth of the deposit stops: and some deposits adsorb, adhere well, and collect further deposits. Therefore, a reasonable hypothesis is that all of the three steps are important for the growth of deposits up to harmful thicknesses.

With this hypothesis as a background, the aim of this work was a deeper understanding of the factors governing the adsorption kinetics

and adhesion of model deposits on different polymer surfaces of relevance to paper machines. The model deposits were chosen to represent typical dissolved and colloidal substances in the circulation water in a paper machine. The study focused on the effect of ionic strength, ion valence, and surface charge on adsorption behaviour. It endeavours to compare the behaviour of the many different types of adsorbates present in paper machine process liquids with respect to polyurethane surfaces, rather than to give a detailed quantitative interpretation of the adsorption mechanism of each adsorbate.

EXPERIMENTAL METHODS

Quartz Crystal Microbalance with Dissipation (QCM-D)

QCM-D Method [14–16]

A quartz crystal microbalance with dissipation (QCM-D from Q-Sense AB, Gothenburg, Sweden) was used. The crystal oscillates at a resonant frequency, f_o, which is lowered to f when material adsorbs on its surface. The shift in this frequency and in several overtone frequencies ($\Delta f = f_o - f$) is measured with a repetition frequency of ≈ 1 Hz. If the adsorbate is evenly distributed, rigidly attached, and small compared with the mass of the crystal, Δf is related to the adsorbed mass by the Sauerbrey equation [17]:

$$\Delta m = -\frac{C\Delta f}{n}, \tag{1}$$

where Δm is the adsorbed mass per unit surface, n is the overtone number (in the present case $n = 1, 3, 5,$ or 7), and C is a constant that describes the sensitivity of the device to changes in mass. The mass calculated in this way also includes the mass of water that has been coupled or trapped in the adsorbed layer [18]. The equation is not valid for viscoelastic layers, for which it may either underestimate or overestimate the adsorbed mass depending on the type of viscoelasticity. Also, it has also been found [19–21] that, if the roughness of adsorbed layer is on the order of hundreds of nanometers or more, surface roughness increases the values of Δf so that the mass of the adsorbed particles in this size range are overestimated.

If the adsorbed material is not fully elastic, frictional losses occurs, which lead to a damping of the oscillation within the material with a decay rate of the amplitude that depends on the viscoelastic properties of the material. With the QCM-D instrument the change in the dissipation factor, $\Delta D = D - D_o$, when material is adsorbed can be measured, where D_o is the dissipation factor of the pure quartz crystal

immersed in the solvent and D is the dissipation factor when material has been adsorbed. D is defined by

$$D = \frac{E_{diss}}{2\pi E_{stor}}, \tag{2}$$

where E_{diss} is the total dissipated energy during one oscillation cycle and E_{stor} is the total energy stored in the oscillation. The decay rate depends on the adsorbed mass and the viscoelasticity of the adsorbed layer. The decay rate is slower for rigid deposits than for viscoelastic deposits.

Useful qualitative interpretation of results can be achieved by plotting ΔD as a function of Δf, as discussed by Höök [22]. If the adsorbed layer is nonslipping, even, and relatively thin, large values for $\Delta D/\Delta f$ indicate that the adsorbed layer is more viscous, while low values of $\Delta D/\Delta f$ indicate a more rigid layer. A large $\Delta D/\Delta f$ may also indicate that the adsorbed layer is very rough. Changes in the slope of the plot of ΔD *versus* Δf indicate changes in the viscoelastic behavior of the adsorbed layer during adsorption.

In the quantitative analysis of data for viscoelastic films, the energy dissipation Equation (2) has to be taken into account. Measurements at several overtones allows the set of data (at $n = 1, 3, \ldots$) to be compared with more complex models. In this article the properties of the adsorbed film are interpreted in terms of the Voigt element (Figure 1) as described by Voinova *et al.* [23]. It is assumed that the adsorbate forms a homogeneous, nonslipping film of uniform thickness d_f and

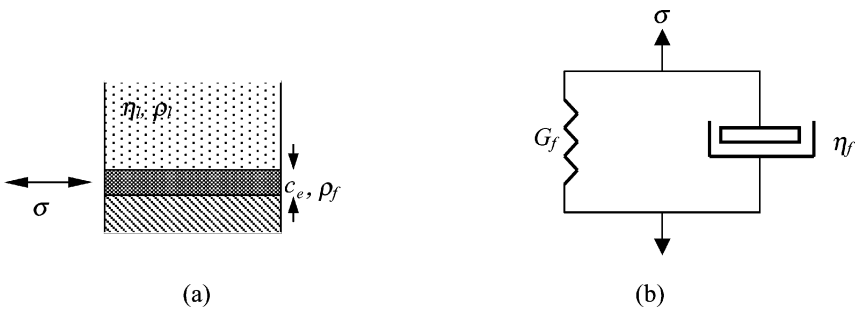

FIGURE 1 Model used for interpretation of viscoelastic properties. (a) A viscoelastic thin film of density ρ_l and thickness d_f is located between the elastic quartz crystal and a viscous solution of viscosity and density ρ_l. (b) The film is subjected to an oscillating shear stress σ and behaves like a Voigt element with a dashpot (shear viscosity η_f) connected in parallel with a spring with shear modulus G_f.

density ρ_f between the QCM-D crystal and a Newtonian liquid of density ρ, and that viscosities and elasticities do not depend on the frequency within the range investigated. The complex shear modulus of the film is defined by

$$G = G' + iG'' = \mu_f + 2\pi i f \eta_f = \mu_f(1 + 2\pi i f \tau_f), \quad (3)$$

where μ_f is the elastic shear (storage) modulus, η_f is the shear viscosity (loss modulus), f is the oscillation frequency, and τ_f the characteristic relaxation time of the film.

Results from measurements at several overtones were fitted to the Voigt model using the program Q-Tools (from Q-Sense Q-Sense AB, Gothenburg, Sweden). Equations connecting ΔD and Δf to μ_f, η_f, the thickness of the film, and the densities of the solvent and the film are given in Voinova *et al.* [23].

Procedure

AT-cut quartz crystals of thickness 0.1–0.3 mm with $f_o \approx 5$ mHz and $C = 0.177$ mg m^{-2} Hz^{-1} were used. The volume of the measurement chamber was 70–100 µl. Before the measurement the polymer substrate was allowed to swell until a stable signal was achieved. An adsorption experiment was started by passing about 500–700 µl of solution through the cell. The total exchange time was 5–30 s, but the time of exchange of liquid adjacent to the crystal is shorter (~1–5 s). After full exchange the inlet valve of the cell was closed and the deposition was recorded in stagnant conditions.

Atomic Force Microscope (AFM)

The AFM instrument was a Nanoscope IIIa multimode scanning probe microscope (Digital Instruments Inc., Santa Barbara, CA, USA). AFM images were scanned in tapping mode in air and in some cases in water using commercial Si cantilevers from Digital Instruments. The resonance frequency of the cantilevers was 400 kHz. A free amplitude (A_o) of about 20 nm and a set-point ratio (r_{sp}) between 0.4–0.6 was used. The ratio between the set-point amplitude (A_{sp}) and A_o is r_{sp}. No image processing except flattening was made. Roughness analysis and flattening were performed using AFM software (Digital Instruments). Four to eight different images were scanned at different locations on each sample. Images deemed representative of the samples were chosen for presentation.

AFM was used to investigate the morphology of the surfaces of some of the QCM-D crystals after adsorption. Before investigation, these

crystals were immersed in distilled water some minutes in order to avoid the precipitation of salt crystals. With some exceptions, AFM studies were made of dried samples.

AFM studies were also made of cross-linked polyurethane surfaces. These were immersed in solutions containing model substances for several hours. Then they were immersed in distilled water for some minutes and dried.

Other Instruments

Contact Angles

A contact angle goniometer (CAM 200, KSV Instruments, Helsinki, Finland) was used.

Zeta Potentials

Electrophoretic mobilities were determined with a Laser-Doppler electrophoretic light-scattering analyzer (Coulter Delsa 440SX, Coulter Co. Lutox, UK). Zeta potentials of polyurethane, AKD, latexes, and wood resin dispersions (all containing particles that, to a good approximation, are spherical) were calculated from electrophoretic mobilities and particle sizes using the Henry equation [24],

$$\zeta = \frac{3u_e\eta}{2\varepsilon f(\kappa a)}, \tag{4}$$

where u_e is electrophoretic mobility, η is the viscosity of water, ε is the permittivity of the solvent, a is the particle radius, κ^{-1} is the Debye length, and $f(\kappa a)$ is the Henry correction factor. Correction factors were taken from Hunter [24].

X-ray Photoelectron Spectroscopy (XPS) Analysis

XPS spectra were recorded with an Axis-165 spectrometer (Kratos Analytical, Manchester, UK) at the Centre for Chemical Analysis, Helsinki University of Technology, using a monochromatic Al Kα X-ray source. All spectra were collected at electron take-off angle of 90° from areas less than 1 mm in diameter. In order to average out the heterogeneities of the samples, scans were recorded from several locations on each sample.

Other methods

Particle sizes and diffusion coefficients were determined by dynamic light scattering (Coulter N4 MD, Coulter Co). A SCS spin-coater (Specialty Coating Systems, Indianapolis, IN, USA) was used

for spin-coating the polyurethane and polyamide substrates. Isoelectric points of cross-linked polyurethane samples were measured with an Electrokinetic Analyzer (EKA; Anton Paar, Graz, Austria).

Substrates

Polyurethane Surfaces

Gold-plated QCM-D-crystals (from Q-Sense AB, Gothenburg, Sweden) were spin-coated with aromatic polyester polyurethane in the following way. The surface of the QCM-D crystal was scratched lightly, to give scratches with an estimated length of several millimeters and width of some hundreds of micrometers. 50–60 μl of a 0.5% dispersion of polyurethane in water, (technical grade, particle size 80–100 nm, containing small amounts of organic additives) was dropped on the surface. The crystal was rotated approximately one minute in the spin-coater at 1500 rpm/min.

The coverage of the surface by polyurethane was verified by AFM and XPS or by visual inspection only. The polyurethane was visible under strong light as a brownish layer on the crystal. Special care was taken to ensure that the spin-coated layer covered the center part of the crystal that is the most sensitive to adsorption.

Before the XPS analysis the crystals were rinsed in distilled water and blown dry with nitrogen. The XPS spectra showed high signals from carbon and oxygen but also of gold amounting to 0.2–2.2 atomic%, being lowest at the center of the crystals. Furthermore, the shape and the relative intensity of the inelastic background of the gold Au 4f photoelectrons clearly indicated that the gold was buried beneath a coating layer [25, 26].

Figure 2 shows an AFM image of the centre part of a QCM-D-crystal coated with polyurethane. The figure indicates coverage of the surface by polyurethane particles with voids between the particles. However, the XPS results verified that there must be at least 2–6 nm of organic substance covering the gold even in the voids. The roughness of the surface (rms R_q) varied between 1.5–6 nm as determined using the standard AFM Nanoscope III 4.43r8 program.

Electrophoretic mobilities of the polyurethane particles in the dispersion used for spin coating were measured at different pHs and in different electrolytes (Figure 3 and Table 1). It was concluded that the isoelectric point of the dispersion was about pH 3.7. At this pH the dispersion coagulates. A maximum in the absolute value of the zeta potential occurs at pH 9–11.

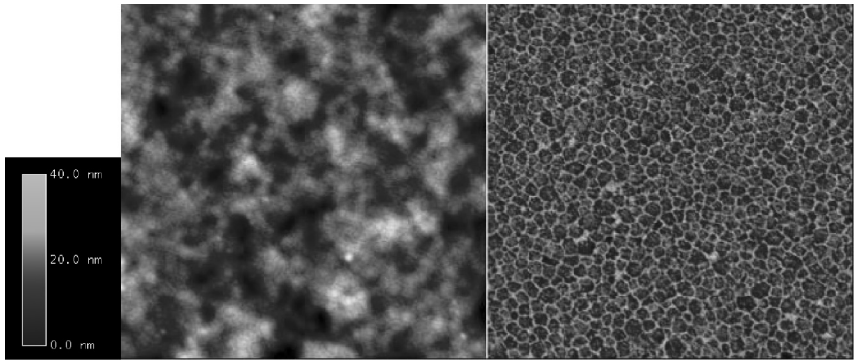

FIGURE 2 AFM image from a spin-coated polyurethane layer. The topography image is to the left and the phase contrast image is to the right. The size of both images is $1.5 \times 1.5\,\mu m$. The thickness of the polyurethane layer is several hundred nm. The rms roughness (R_g) of the polyurethane layer is around 3 nm, as evaluated from the topography measurement.

Contact angles of dry and wetted polyurethane-coated QCM-D crystals were measured (Table 2). After wetting, the surfaces were blown dry with nitrogen and the contact angle was measured immediately.

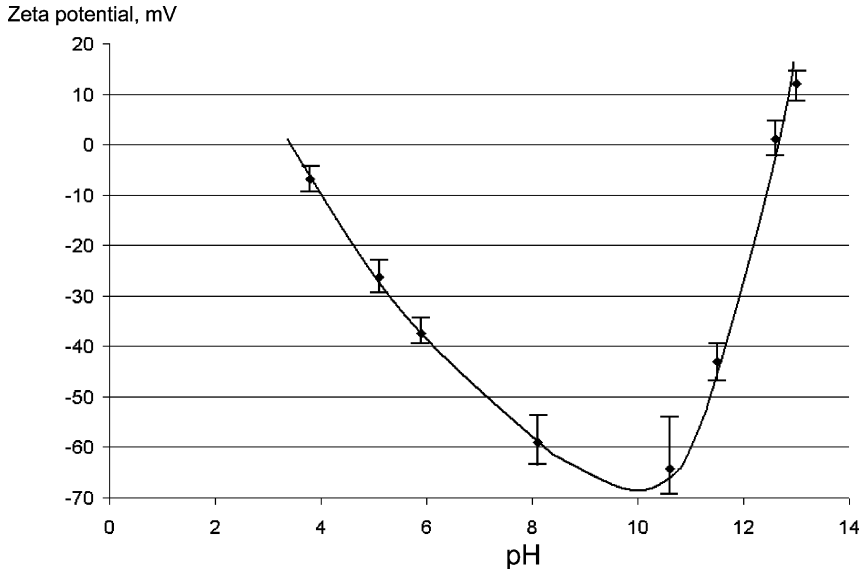

FIGURE 3 Zetapotential of polyurethane dispersed in 0.1 mM NaCl as a function of pH.

TABLE 1 Electrophoretic Mobilities and Zeta Potentials of Polyurethane Particles in Different Electrolytes at pH 7

Electrolyte	Mobility $\mu m\ s^{-1}\ V\ cm^{-1}$	Zeta potential mV
0.1 mM NaCl	−2.6	−51
10 mM NaCl	−2.2	−29
1 mM $CaCl_2$	−1.4	−20
10 mM $CaCl_2$	−1.0	−12
1 mM Na_2SO_4	−0.2	−3
10 mM Na_2SO_4	0.6	+7

Spin-coated polyurethane layer swelled, especially at high salt concentrations (100−500 mM NaCl). Due to swelling, the frequencies in QCM-D typically decreased a few dozens of hertzes in tens of minutes at high salt concentrations.

Cross-linked polyurethane

Two samples of cross-linked polyurethane were investigated (samples D1 and A3; Table 3). Sample D1 was prepared from the same polyurethane as the dispersion used in QCM-D experiments. The only difference was that the sample had been cross-linked to some extent by heating. Sample A3 contained the same polyurethane as D1, ceramic filler particles, some additives, and a surfactant. A3 is used in paper machines.

AFM analysis showed that sample D1 and the polyurethane part of sample A3 consisted of roughly spherical polyurethane particles similar to the spin-coated polyurethane surface used in QCM-D experiments. The diameter of the particles was 30−120 nm. The rms (Rq) values of the surfaces were 8−25 nm for both D1 and the polyurethane part of A3. The ceramic filler was extremely flat with some nanometer variations in height only. Large changes in height (some micrometers

TABLE 2 Contact Angles of Water on Spin-coated Polyurethane Layer

Treatment	Contact angle	Type of contact angle
Dry	63−66°	Static
Dry	66−72°	Advancing
Wetted several hours in distilled water	70−72°	Advancing
Wetted with 10 mM NaCl	70−72°	Advancing
Wetted with 100 mM NaCl	70−72°	Advancing

TABLE 3 Contact Angles, Isoelectric Points and Charges in Distilled Water of Cross-linked Polyurethane

Sample	Composition	Advancing contact angle (wet)	Advancing contact angle (dry)	Isoelectric point pH	Surface charge at pH 7
D1	Crosslinked polyurethane	60–64°	75–77°	3.6	anionic
A3	Crosslinked polyrethane with ceramic filler, additives and surfactants	75–88° depending on drop size and shape	62–78°	3.9	anionic

or more) were recorded at the borderlines between ceramic filler and polyurethane.

The high roughness and heterogeneity of the surface rendered the contact angles of samples A3 and D1 highly dependent on the size and the shape of the drop. For this reason the contact angle measurements were rather scattered.

Polyamide surfaces

Gold-plated QCM-D crystals were spin-coated with a 0.5% solution of polyamide in formic acid (Polyamide 6, analytical grade). Formic acid was removed by freeze-drying the spin-coated crystals for several days before adsorption experiments. The surface was several hundred nanometers thick, as estimated with AFM, but thin enough to work well in QCM-D measurements. The properties of the surface were assumed to be similar to those of the surfaces described in Kekkonen *et al.* [27] and Kekkonen [28].

Adsorbates

Properties of the adsorbates investigated are summarized in Table 4.

Kaolin and Talc

The kaolin clay contained small amounts of Na_2CO_3 as well as sodium polyacrylate as a dispersant. Colloidally stable kaolin was prepared as decribed in Goodwin *et al*. [29]. A dispersion of kaolin was thoroughly stirred and allowed to sediment several days in a large vessel. The part of the dispersion that had not sedimented was separated and used in the experiments. The talc dispersion was prepared

TABLE 4 Properties of Adsorbates

Adsorbate	Supplier	Particle size/molar mass	Zetapotential and charge densities	Notes
Cationic				
AKD-wax	Raisio Chemicals	350–360 nm	24 mV (0.1 mM NaCl, pH 7)	Wax-content of the particles was about 50%
C-PAM	Allied Colloids, Hydrocol 880	$5.6 \cdot 10^6$	0.97 mmol/g (pH 7)	
Cationic starch (pH 5.5–7)	Raisio Chemicals	Several millions but less than native starch		Degree of substitution 0.038; amount of nitrogen 0.315%
Anionic				
Talc	Finntalc M03	600–700 nm		
Kaolin	Thielekaolin	400–500 nm		
Polystyrene latex	Prepared as described in [37]	225–260 nm	– 39 mV (0.1 mM NaCl, pH 7)	
CMC	Metsa Specialty Chemicals	$2 \cdot 10^5$		Degree of substitution 0.57
Wood resin droplets (pH 5.5)	Prepared as described in Crank [38]	135–265 nm	– 48 mV (0.1 mM NaCl, pH 5.5)	
Nonionic or very weakly ionic				
Polyethylene oxide	Seitetsu Kagaku	$5–6 \cdot 10^6$		
PVA	Hoechst AG	$2.7 \cdot 10^4$		Degree of hydrolysis 98%
Native starch	Raisio Chemicals	Several millions		Raw material for cationic starch (see above)

in the same way. The concentration of dispersions used in the experiments was 0.1 g/l. At the pH values used in this study the net charge of the kaolin and talc particles will be negative [29].

Cationically Modified Polyacrylamide (C-PAM)

The solution of C-PAM was prepared as described by Swerin *et al.* [30, 31]. First, 0.1 g C-PAM was wetted with 2 ml ethanol in a 200 ml flask for some minutes. Water was added and the flask was shaken several minutes. The solution was stirred and left overnight without stirring. After stirring the solution was diluted to 0.1 g/l.

Carboxymethyl Cellulose (CMC)

The degree of polymerisation of CMC was 1700 and its molecular mass was 200 000, according to data given by the manufacturer and Brookfield viscosity measurements.

Cationic Starch (CS)

Wax maize starch was cationised at the laboratories of Raisio Chemicals, Rasio, Finland, by substitution with 2,3-epoxypropyltrimethylammoniumchloride. 0.1 g/l starch was dissolved in 10 mM NaCl by stirring at 90°C for 10 min and then overnight at 50–60°C.

Alkyl Ketene Dimer (AKD) Wax Dispersions

A 20% (10% active wax) AKD dispersion (Raisio Chemicals, Raisio, Finland) that was sterically stabilised and contained cationic starch was diluted to 0.1 and 0.5 g/l. The softening point of the wax was around 48°C.

Model Emulsions

Emulsions of wood resin with electrostatic stabilization were prepared according to the method described by Sundberg *et al.* [32]. Unbleached thermomechanical Norway spruce (*Picea abies*) pulp (TMP) was obtained from a Finnish paper mill and was stored in a freezer at −24°C until used. Freeze-dried TMP was extracted with hexane in a Soxhlet apparatus. After extraction the hexane was evaporated and the resin was dissolved in acetone. The solution was filtered and injected in water under stirring. Finally, the acetone was removed by dialysis. It has been suggested that wood resin droplets in paper mills are usually covered by a sterically stabilizing layer of hemicelluloses [4, 33]. However, it can be argued that in a fouling situation the layer of hemicelluloses is inadequate, and thus the model emulsion used in this study is thought to resemble "fouling wood resin." The zeta potential and particle size measured for the resin droplets (Table 4) agreed

TABLE 5 Results from Adsorption Measurements

Substance, conc. 0.1 g/l[5]	Electrolyte conc. mM[1]	Δf/1 min Hz	Δf/final Hz	Time to ads. plateau min	$\Delta D_{sat}/\Delta f_{sat} \cdot 10^9$ (end of ads.)	Ads. amount $\mu g/cm^2$
Cationic substances						
AKD	0.1	105	160	20	35–40	
	10	50–70	395	50–60	50–70	
	100	None/very slow	150	80–150	50	
	100 mM Na_2SO_4	None very slow				
0.5 g/l	0.1	240				
C-PAM	10	80	250–280	>250	30–35	1.5–1.7
Cat. starch	10	150	340–370	>400	33–37	2–2.2
	10 (pH 5.5)	8	20	30		
	100	23–28	160	280	65–70[2]	
	300	None/very slow				
	7.5 mM $CaCl_2$	76.5	168	19	70	
	10 mM Na_2SO_4	140	>270	30	45–46	
	100 mM Na_2SO_4	7.5	14–15	>20	100	
Anionic substances						
Talc	10	20	200	>500	70	
	100	None/very little				
Kaolin	0.1	None				
	10	None				
	20	2	280	>500	95–100	
	50	Large		Medium		
Polystyrene latex	0.1	None				
	1	None				
	10	1	500–530	>5000	180–190	
	10 + flow	—	>1500	120	50–60	
	100	40	>800	>600	70	
	4	71	1700	1000	40	

Wood resin (pH 5.5)	0.1	5–10	5–10	1–2 (135 nm)	
	10	54	166	50 (150 nm)	85–90
	100	38	230	500–600 (286–700 nm)	22–27
	300[2]	None/very little			
	1 mM $CaCl_2$	27	>210	>200	25–30
CMC	10	No adsorption			
Nonionic polymers					
PEO	10	No ads.			
Native starch	10	No ads.			
PVA	10	Negligible			

[1]NaCl (if not stated otherwise).
[2]10–300 min. Decreases after 400–1000 min to $\approx$40.
[3]Aggregated, particle size 850–4000 nm.
[4]0.1–0.3 mM NaCl, 0.1 mM $CaCl_2$.
[5]Unless otherwise stated.
Reproducibility of Δf, ΔD, and $\Delta D_{sat}/\Delta f_{sat}$ usually $\pm$10–20%.
Adsorbed amounts calculated using Equation (1).
pH = 7 unless otherwise stated.

well with earlier studies [34]. The concentration was 0.1 g/l in all experiments.

Other Reagents

All solutions and dispersions were prepared with distilled water. Analytical-grade NaCl, $CaCl_2 \cdot 2H_2O$, or $Na_2SO_4 \cdot 10\,H_2O$ was used. Small amounts of HCl and NaOH were used to adjust the pH.

Choice of Experimental Conditions

Experiments with QCM-D were made mainly at pH 7 and different salt concentrations (0–500 mmol/l NaCl, 0–1 mM Ca^{2+}, and 0–1 mM SO_4^{2-}). The concentration of adsorbates was 0.1 g/l in most experiments. The representative of conditions in modern paper mills are 0.1 g/l adsorbates, pH 7, and 10–100 mM NaCl [9]. Calcium and sulfate ions are also commonly present in circulation waters, and changes in their concentration often cause fouling. The concentration 0.1 g/l is low enough so that the viscosity increase due to dissolved polymers can be neglected. However, it is also so low that in batch experiments significant depletion of colloidal adsorbates in the sample chamber may occur towards the end of the adsorption experiments. With initial concentration of 0.1 g/l, the amount of colloidal material in the chamber is around 10 μg. If the adsorbed amount is 2 μg (as with cationic starch; see Table 5), the concentration inside the chamber may decrease as much as 50% because adsorption takes place not only on the QCM-D crystal but also on gaskets and steel parts.

RESULTS

Cationic Substances

Cationic starch adsorbed rapidly on the polyurethane-coated QCM-D crystal at pH 7 and low ionic strength (Figure 4), *i.e.*, from 10, 100 mM NaCl, 7.5 mM $CaCl_2$, and 10 mM $NaSO_4$. However, no adsorption took place from 100 mM $NaSO_4$ or from 300 or 500 mM NaCl. Adsorption at pH 5.5 was very slow. AKD-wax particles, which are rendered cationic by adsorbed cationic starch, adsorbed rapidly from 0.1 mM NaCl and 10 mM NaCl but much slower from 100 mM NaCl and 100 mM Na_2SO_4. C-PAM adsorbed rapidly from 10 mM NaCl.

AFM imaging (Figure 5) showed that cationic starch forms an even layer on polyurethane. AKD wax adsorbs as scattered particles on the

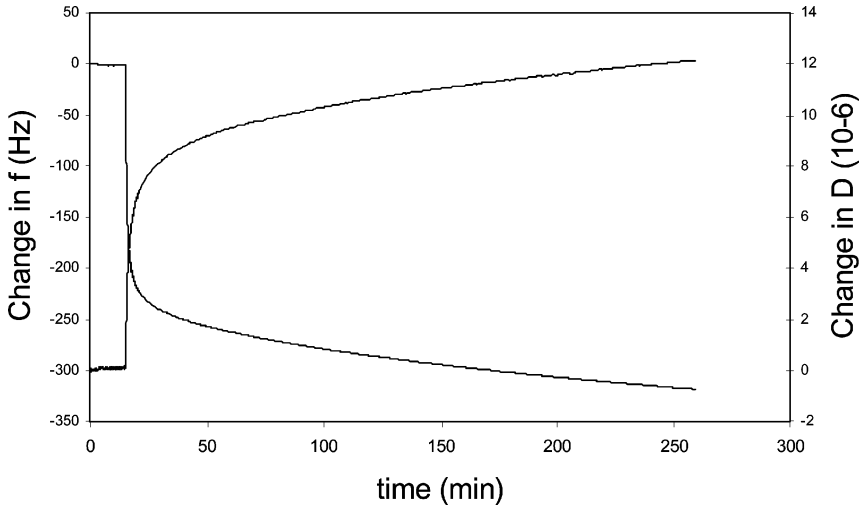

FIGURE 4 Adsorption of cationic starch on a polyurethane-coated QCM-D crystal from a 0.1 g/l solution in 10 mM NaCl at pH 7. The decreasing curve shows the change in resonance frequency as more material is adsorbed. The rising curve shows the concomitant change in dissipation. The sharp break indicates the moment at which water in the cell was replaced by the starch solution.

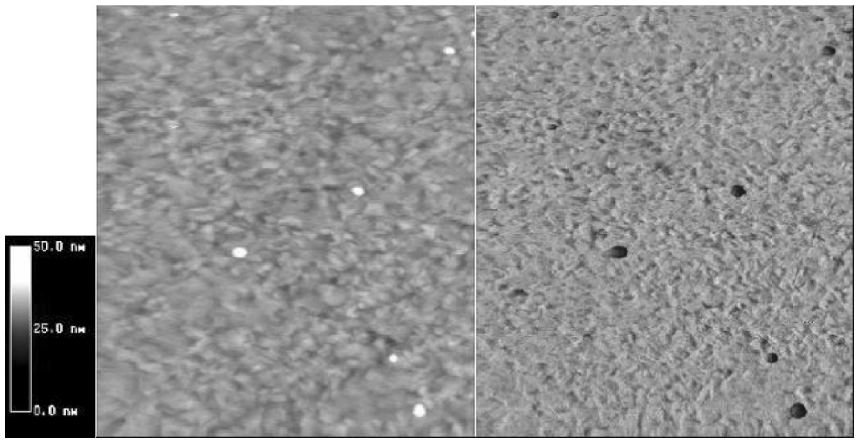

FIGURE 5 Representative AFM-images ($3 \times 3\,\mu m$) of an adsorbed layer of cationic starch. The topography image is to the left and the phase contrast image is to the right. The measurement was made with the surface immersed in water. Note that the topography of the adsorbed layer to some extent reproduces the morphology of original polyurethane layer.

surface. The particles spread on the surface so that a large contact area is created (Figure 6).

These results show that electrostatic and van der Waals interactions control the adsorption (heterocoagulation) of these cationic substances. Increasing the ionic strength screens the electrostatic attraction between the negatively charged surface and cationic particles and, thus, cationic starch and AKD-wax do not adsorb at higher salt concentrations. At pH 5.5, electrostatic attraction is weaker due to the decrease in surface charge of polyurethane.

The role of van der Waals interactions should also be considered. For attractive van der Waals forces to be negligible in aqueous solution, the Hamaker constant of either adsorbent or adsorbate need to be similar to or smaller than that of water 35. The Hamaker constants for polyurethane or the cationic polymers have not been determined. However, it has been reported that the Hamaker constants for polymers are somewhat larger than the Hamaker constant of water unless the material contains large amounts of fluorine [12, 36, 37]. Therefore, attractive van der Waals forces most likely occur between the polyurethane surface and the adsorbates used in this study, but they apparently are too weak to induce significant adsorption or lead to adsorption that is too low to be detected by QCM-D if electrostatic double-layer attraction is screened.

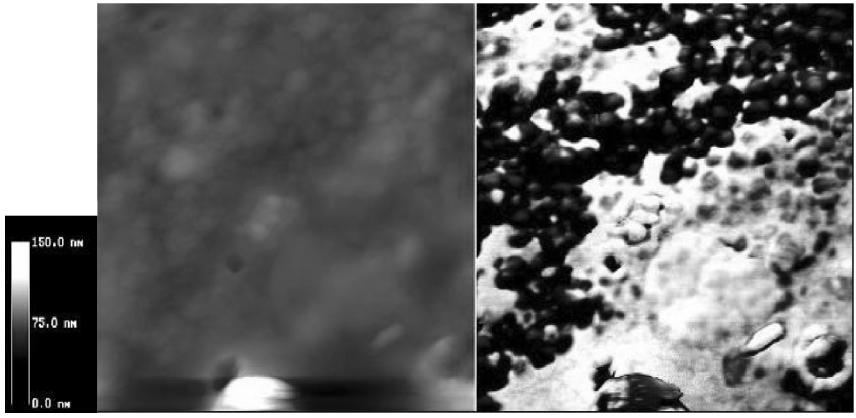

FIGURE 6 Representative AFM images of adsorbed AKD particles (0.5 g/l, pH 7, 10 mM NaCl). Topography image is to the left, phase contrast image is to the right, both images $1 \times 1\,\mu m$. In the phase contrast image the tone is lighter the softer the material, thus the soft AKD is white and the harder polyurethane dark gray.

As predicted by the DLVO theory of colloidal stability, addition of divalent simple ions (sulphate) screens electrostatic interactions more effectively than monovalent ions (chloride) at the same concentration.

Anionic Substances and Non-ionic Polymers

Kaolin and polystyrene latex did not adsorb at low salt concentrations. Polystyrene latex began to adsorb when the NaCl concentration was raised above 1–1.5 mM. The rate and the amount of adsorption were slightly higher from slowly flowing (0.8 ml/min) dispersion (Figure 7) than under stagnant point conditions (see Table 5). As discussed above, depletion of the solution in the chamber during the measurement may reduce adsorption if there is no flow. Polystyrene latex adsorbed as discrete particles (Figure 8). The size of the latex particles was slightly smaller in the experiment with the flow because a different batch of polystyrene latex was used.

Like polystyrene latex, kaolin did not adsorb from 0.1 mM NaCl. Adsorption started at NaCl concentrations above 10–12 mM (Figure 9).

Talc adsorbed slowly from 10 mM NaCl and 100 mM NaCl. It adsorbed unevenly in pile-like formations (Figure 10). Its adsorption behavior did not seem to be related to electrostatics. The dispersion was not very stable. Therefore, the piles are probably aggregates that have formed in the solution.

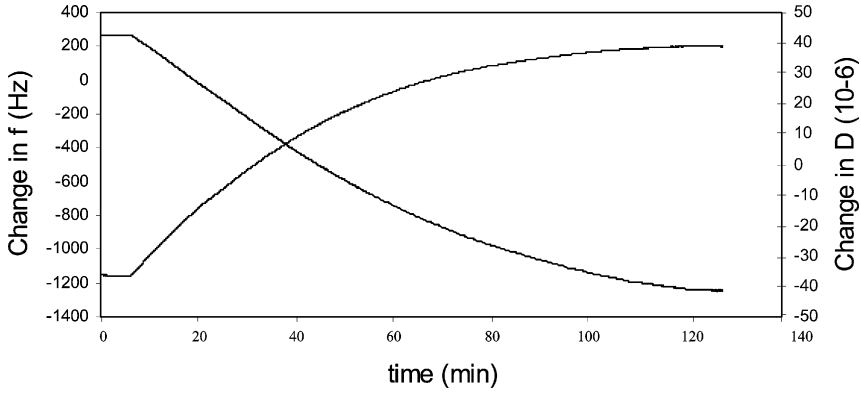

FIGURE 7 The adsorption of polystyrene latex on a polyurethane-coated QCM-D crystal from 0.1 g/l dispersion in 10 mM NaCl at pH 7. The decreasing curve shows the change in resonance frequency and the rising curve the change in dissipation. The dispersion flowed through the cell during the experiment (0.8 ml/min).

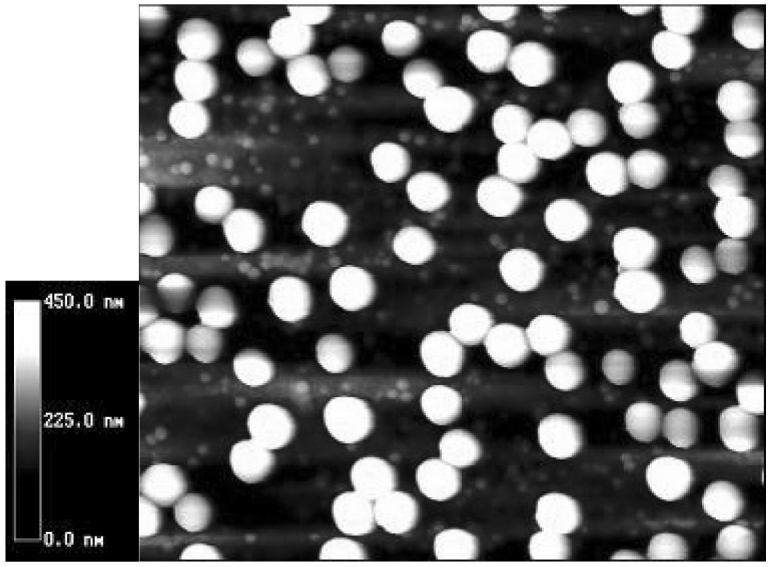

FIGURE 8 Topographic AFM image (size $6 \times 6\,\mu m$) of polystyrene latex that adsorbed in the process illustrated by Figure 10. Most of the polystyrene particles are flattened. Their diameter is 350–410 nm, and the height is around 200–260 nm.

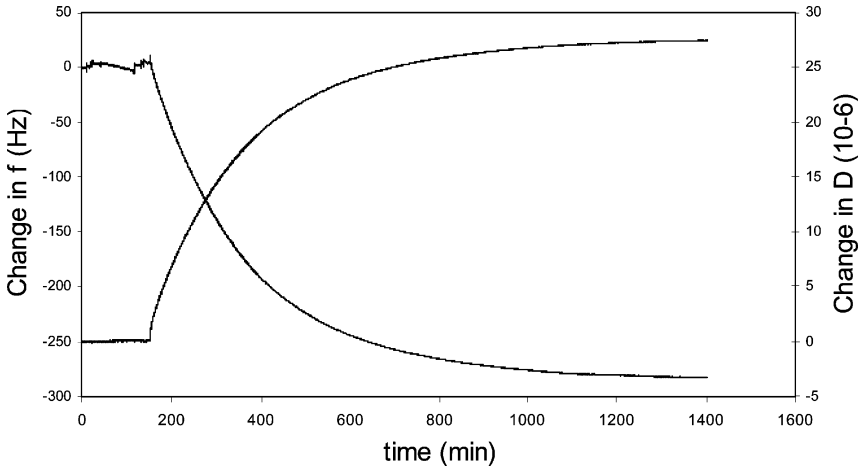

FIGURE 9 Adsorption of 100 mg/l kaolin dispersion in 20 mM NaCl at pH 7 on a polyurethane-covered QCM-D crystal. The decreasing curve is change in resonance frequency, and the rising curve is change in dissipation.

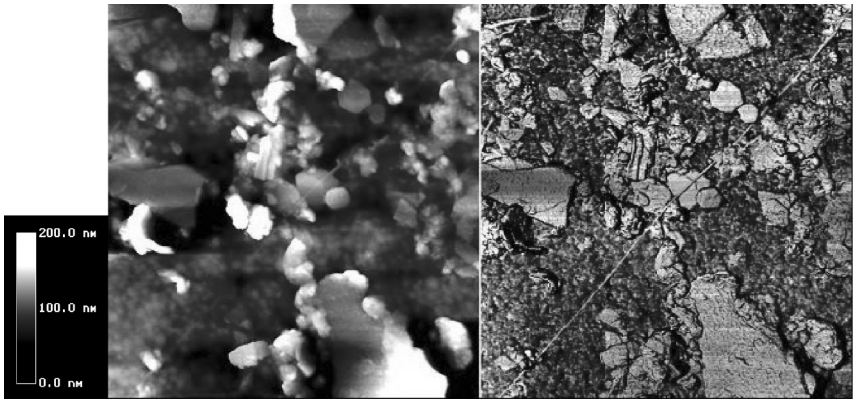

FIGURE 10 AFM topography image (left) and phase contrast image (right) of adsorbed talc particles on polyurethane. The size of both images $3 \times 3\,\mu m$.

As with cationic substances, these results indicate that the adsorption is primarily governed by van der Waals and electrostatic forces. Electrostatic repulsion between anionic substances and anionic surface prevents adsorption when the ionic strength is low enough.

As mentioned earlier, the Sauerbrey equation overestimates the mass of the adsorbed particles if the surfaces are very rough. From the AFM micrograph (Figure 8) it can be estimated that the adsorbed mass of polystyrene latex is around 4 times as large as that estimated by Equation (1). Table 5 shows that $\Delta D/\Delta f$ values for the polystyrene latex, kaolin, and talc are relatively high. We suggest that this is a result of both the roughness of the adsorbed layer and trapping of the water in cavities between the adsorbed particles and polyurethane surface.

In the experiments with wood resin the emulsion pH was 5.5. No adsorption took place from 0.1 mM NaCl. Adsorption from 10 mM NaCl was slightly faster than from 100 mM NaCl (Figure 11) and 1 mM $CaCl_2$, where the droplets were slowly coagulating. An interesting observation was that adsorption on polyurethane was almost negligible at very high salt concentrations (300 mM NaCl), where the pitch droplets were strongly coagulated. The $\Delta D/\Delta f$ values in 10 mM NaCl were higher than in 100 mM NaCl and 1 mM $CaCl_2$. This suggests that the resin droplets do spread on the surface at 10 mM NaCl but remain as scattered droplets on the surface, presumably due to electrostatic repulsion between them at this low ionic strength.

No adsorption of native starch, polyethylene oxide or PVA from 10 mM NaCl was detected.

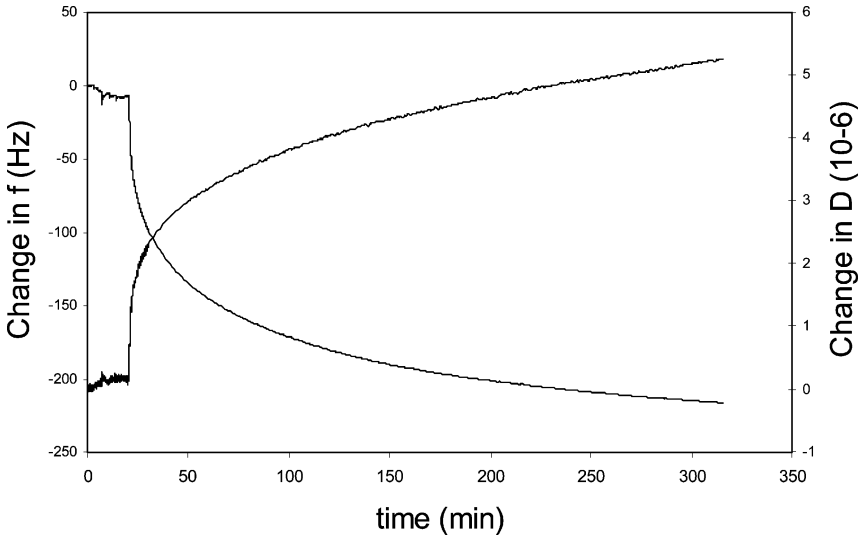

FIGURE 11 Adsorption of coagulating wood resin droplets (concentration 0.1 g/l) on polyurethane (pH 5.5, 100 mM NaCl). The decreasing curve is change in resonance frequency and the rising curve is change in dissipation. The size of the droplets was 284–700 nm during the measurement.

Sequential Adsorption

In experiments with sequential adsorption, first a solution containing a cationic or anionic substance was added to the measurement chamber. When the adsorbed amount had reached a more or less stable plateau level, the chamber was rinsed with water containing the same concentration of salt at the same pH as in the solution containing the adsorbent. A solution containing the oppositely charged substance was then added to the chamber. When the adsorption of this substance reached a plateau level, the chamber was rinsed and the first solution was added again. This was repeated several times in some experiments.

As shown in Figures 12–16, anionic and cationic substances adsorb sequentially on both polyamide and polyurethane.

AFM pictures (Figures 17–19) indicate that the colloids mainly adsorbed as discrete particles on polyurethane. Some pile-like formations, where colloids appear together, can also be found. A large part of the surfaces remains, however, uncovered. Adsorption of kaolin that had already ceased continued when more kaolin dispersion was added

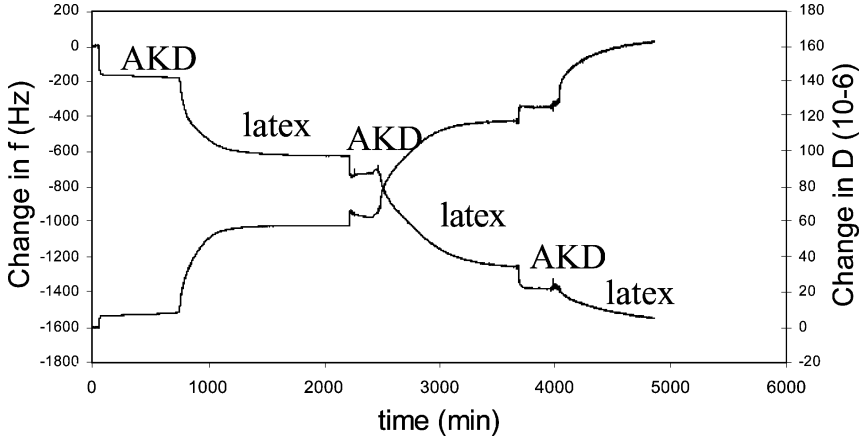

FIGURE 12 Sequential adsorption of AKD wax (100 mg/l) and polystyrene latex (100 mg/l) on polyurethane (pH 7, 0.1 mM NaCl). The sharp breaks in the curves indicate addition of AKD or polystyrene dispersion.

to the chamber (Figure 14). The initial amount of kaolin was 10 μg (0.1 g/l in the volume of 100 μl). According to Equation (1), 9.1 μg kaolin was adsorbed.

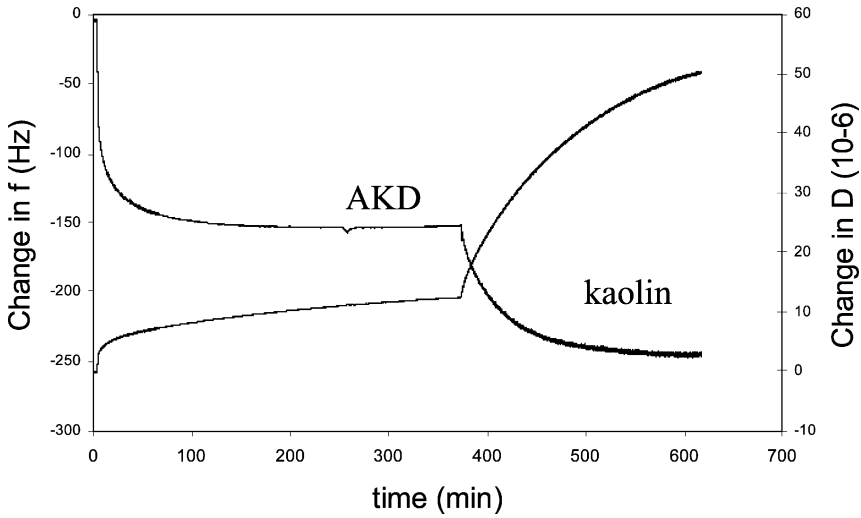

FIGURE 13 Sequential adsorption of AKD (100 mg/l) and kaolin (100 mg/l) on polyurethane (pH 7, 10 mM NaCl).

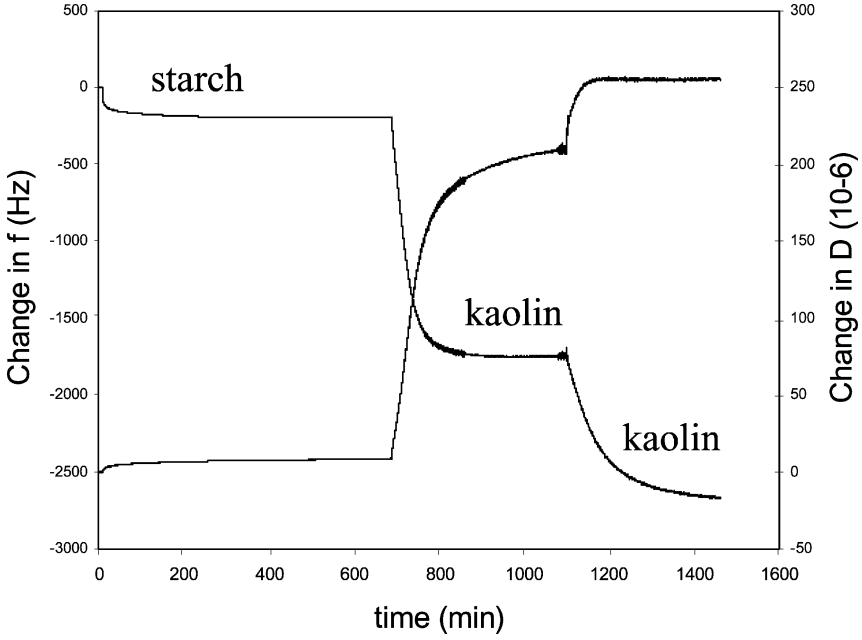

FIGURE 14 Sequential adsorption of starch (0.1 g/l) and kaolin (0.1g/l) on polyurethane (pH 7, 10 mM NaCl).

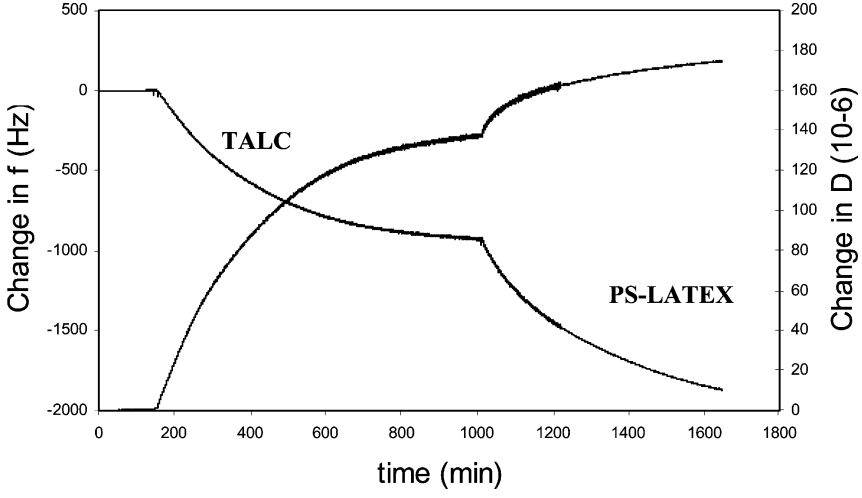

FIGURE 15 Sequential adsorption of talc (0.1 g/l) and polystyrene latex (0.1 g/l) on polyurethane (pH 7, 10 mM NaCl).

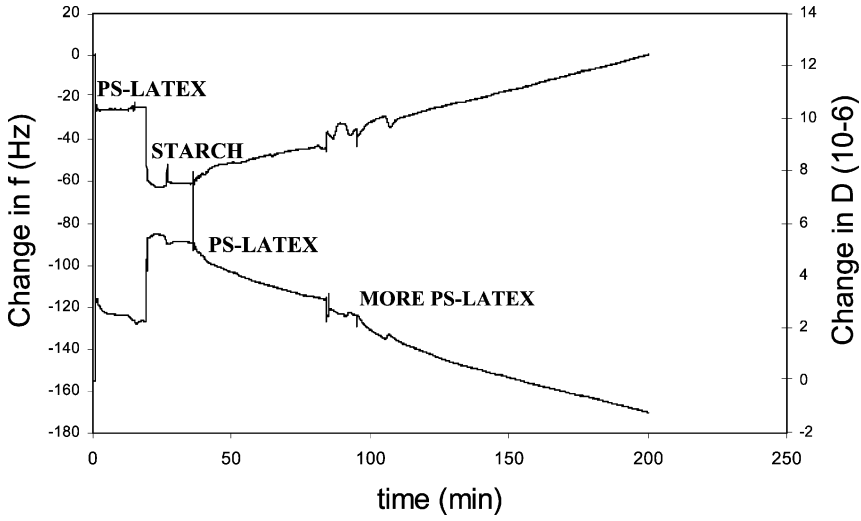

FIGURE 16 Sequential adsorption of polystyrene latex (0.1 g/l, pH 6.8, 0.1 mM NaCl) and cationic starch (0.1 g/l, 0.1 mM NaCl, pH 6,1) on polyamide.

Besides adsorbing on polyurethane, kaolin probably adsorbed on steel and on the O-ring surface inside the chamber. Although the Sauerbrey equation overestimates the adsorbed amount, it is clear that the reason for the continued adsorption when more kaolin was added is that the solution was depleted during the previous adsorption of kaolin.

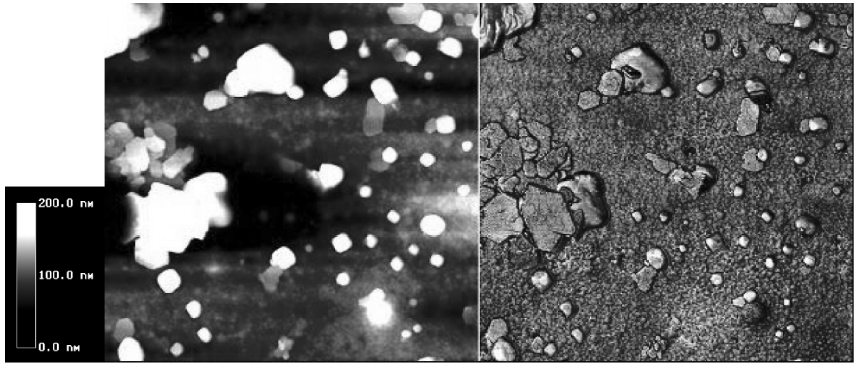

FIGURE 17 AFM-topography image (left) and phase contrast image (right) of adsorbed AKD and kaolin particles (adsorption process illustrated in Figure 13). The size of both images is $6 \times 6\,\mu m$.

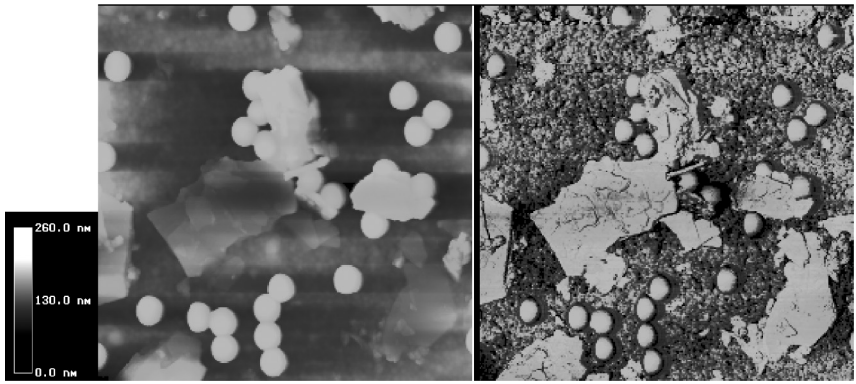

FIGURE 18 AFM topography image (left) and phase contract image (right) from the adsorbed talc and polystyrene latex particles. The size of both images is $5 \times 5\,\mu m$. Latex particles are apparently flattened as in Figure 8.

$\Delta D/\Delta f$ Plots and Viscoelasticity

Values for $\Delta D/\Delta f$ calculated from the final stage of the adsorption experiments are given in Table 5.

The $\Delta D/\Delta f$ graphs for most substances were linear or slightly curved. An example of a $\Delta D/\Delta f$ curve for cationic starch is given in

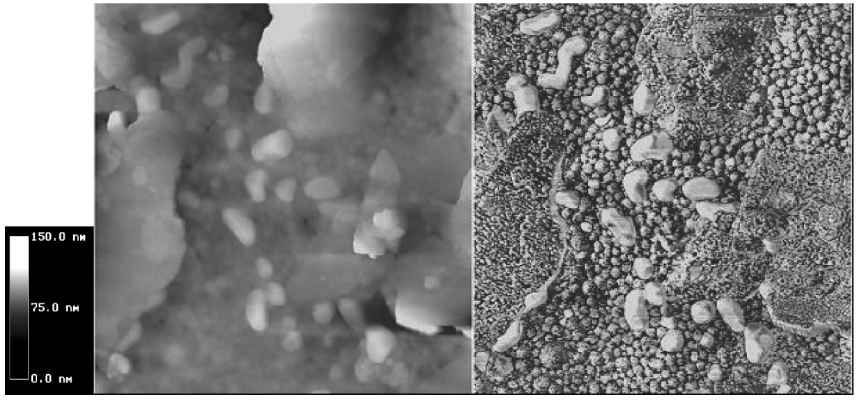

FIGURE 19 AFM topography image (left) and phase contract image (right) of adsorbed AKD and talc particles. The size of both images is $3 \times 3\,\mu m$. pH 7 and 10 mM solution of NaCl with 0.1 g/l concentration of the adsorbing substances was used in the experiment. AKD adsorbed in tens of minutes and talc in hours.

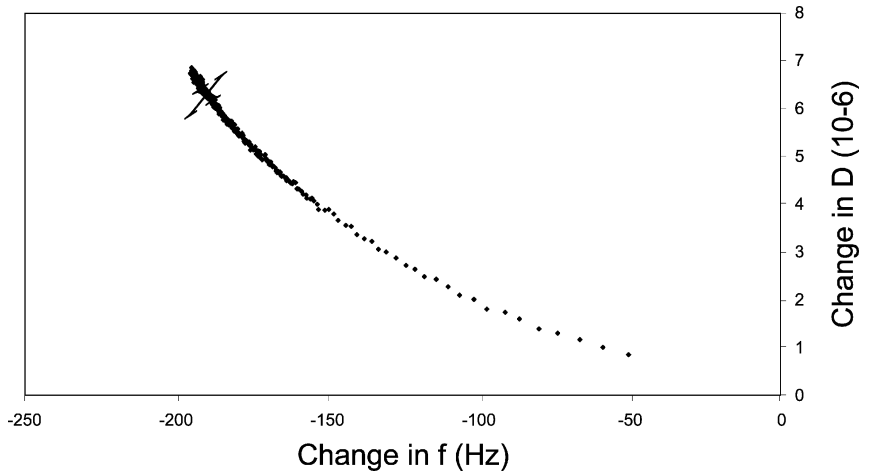

FIGURE 20 Change in dissipation *versus* change in frequency during adsorption during adsorption of cationic starch (0.1 g/l, 10 mM, pH 6.8).

Figure 20. A marked dependence of the slope of the $\Delta D/\Delta f$ curve on time was observed only with talc. Possible reasons for this are that gas bubbles adsorb together with talc and changes in the structure of the adsorbed talc layer.

$\Delta D/\Delta f$ values give relevant information about the viscoelasticity of adsorbed layers of cationic starch and C-PAM, which forms relatively evenly distributed thin films that presumably oscillate without slip. The viscoelasticity of cationic starch is higher and the adsorbed layer is, therefore, less rigid in 100 mM NaCl, 100 mM Na_2SO_4, and in 7.5 mM $CaCl_2$ than in 10 mM NaCl (Table 5). Equation (1) can be used to estimate roughly the mass of cationic starch and bound or trapped water adsorbed from 10 mM NaCl.

The $\Delta D/\Delta f$ plots curve slightly for both cationic starch (Figure 20) and C-PAM. This indicates that changes in the viscoelasticity and/or in the amount of bound or trapped water take place during the adsorption. A slow increase in frequency, decrease in dissipation, and decrease in $\Delta D/\Delta f$ (from $65-70\cdot10^{-9}$ to around $40\cdot10^{-9}$) was detected for cationic starch in 100 mM NaCl after 400–500 min. This indicates that ions and water are forced out from the adsorbed layer.

The properties of the cationic starch layer in 10 mM NaCl was analysed in terms of the Voigt model using Q-Tools. The density of the adsorbed layer was assumed to be 1300 kg/m^3 when the modelling was performed. This assumption had influence mainly on the modelling results with layer thicknesses. The calculated viscosity of the

layer was rather low (0.0016−0.0024 Ns/m^2) and the calculated elastic shear modulus rather high (200,000−440,000 N/m^2) near the end of adsorption. The thicknesses estimated with the Q-tools modelling were near those calculated with Equation (1) (15−20 nm). It was also found that the viscoelastic behaviour of the starch is frequency dependent. Application of the model using the 3rd and 5th overtone gave 0.4−0.5 times smaller values for shear modulus, 1.7−1.8 times larger values for viscosity, and 1.2 times larger values for layer thickness than using the 5th and 7th overtone.

Q-Tools was unable to give an unequivocal value for the shear modulus for the starch adsorption at 100 mM. The adsorption behaviour of starch at this salt concentration seems to be too complicated to be modelled with the rather simple Voight model.

Experiments with Cross-linked Polymer Surfaces

Adsorption on the cross-linked samples A3 and D1 (Table 6) was generally similar to adsorption on the samples containing unmodified polyurethane (Table 5). The contact area of AKD-wax on sample D1 (Figure 21) was as high as on unmodified polyurethane (Figure 6). However, some differences were observed. The amounts of cationic substances adsorbed from similar solutions were smaller than on unmodified polyurethane. The reason is not clear but may be due to changes in charge density and morphology due to cross-linking.

Adsorption on the ceramic filler in the A3 sample was quite different from adsorption on the polyurethane part. PS-latex (0.1 g/l) adsorbed very unevenly on sample A3. Some parts of the polyurethane were rather well covered, while other parts stayed totally uncovered. It seems that for some reason the adsorption properties of the polyurethane are affected by the filler particles-which are located close to the polyurethane that did not adsorb.

DISCUSSION

Diffusion-Controlled Adsorption of Colloids

The rate of adsorption of colloids in stagnant point conditions is often controlled by diffusion. If each individual particle adheres to the surface upon collision with the surface, independently of other adsorbed particles, the amount adsorbed is [38]

$$M_t = 2C_0\sqrt{\frac{Dt}{\pi}}, \tag{5}$$

TABLE 6 Results from AFM Experiments with Cross-linked Polymer Samples

Adsorbate g/l	NaCl mM	Adsorbed amount on	
		Polyurethane	Ceramic filler
Sample A3			
AKD			
0.1	0.1	Some	None or very little
0.5	0.1	Some	None or very little
0.5 (heated to 50–60°C)	0.1	Some	
PS-latex			
0.1	100	Some and very uneven	None or very little
1	100	Large amounts (at least a monolayer)	Presumably a lot
Cationic starch			
0.1	10	Lots	None or very little
Kaolin			
0.1	10	None or very little	
	100	Some	
1.0	100	Lots	
Sample D1			
AKD			
0.1	0.1	Some	
0.5	0.1	Some	
0.5 (heated to 50–60°C)	0.1	Some	
PS-latex			
0.1	100	Lots	
1	100	Lots (at least a monolayer)	
Cationic starch			
0.1	10	Lots	
Kaolin			
0.1	10	None or very little	
0.1	100	Some	
1.0	100	Lots	

where M_t is the concentration of diffusing substance that has left the dispersion at time t, C_0 is the bulk concentration (assumed to remain constant), and D is the diffusion coefficient. The equation holds only in the beginning of the adsorption, because at later stages already-adsorbed particles retard further adsorption. Hence, the adsorbed amounts of particles were calculated only for the first 60 s of adsorption.

Values for M_t estimated from diffusion coefficients measured in salt-free solutions by dynamic light scattering are compared with results from the QCM-D experiments in Table 7. The QCMD-D values are probably too high because the use of Equation (1) tends to overestimate adsorption of large particles that give rise to rough surfaces.

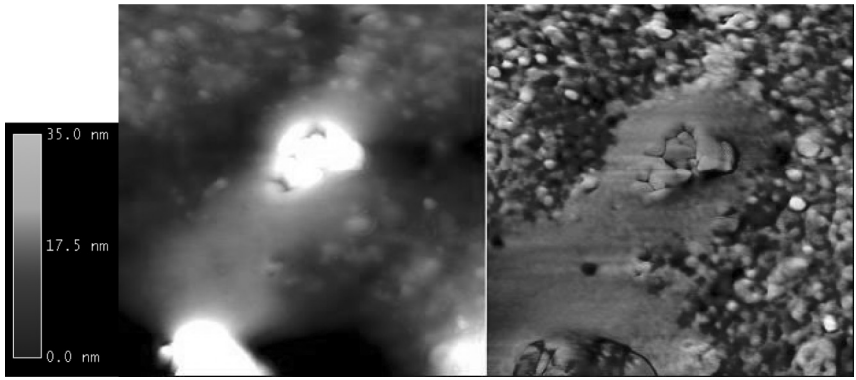

FIGURE 21 AFM topography image (left) and phase contrast image (right) of adsorbed AKD wax particles on surface D1. The size of both images is $1 \times 1\,\mu m$. The polymer parts of the particles can be seen as rises in left image (show as white). The wax part can best be seen in right image as large light area around polymer bulges.

TABLE 7 Calculated and Observed Amounts (by QCM-D) of Adsorbed Particles

		Amount adsorbed after 1 min ng/cm^2	
C_0/salt conditions	D cm^2/s	Calculated from Equation (9)	Calculated from Equation (1)
AKD	1.10^{-8}		
0.1 g/l/0.1 mM NaCl		43.6	619.5
0.5 g/l 10 mM NaCl		217.9	1416
0.1 g/l/ 10 mM NaCl		43.6	395.3
Kaolin	$8.7{\cdot}10^{-9}$		
0.1 g/l/ 20 mM NaCl		81	8.85
Polystyrene latex	$2.1{\cdot}10^{-8}$		
0.1 g/l/ 10 mM NaCl		63.3	5.9
0.1 g/l/ 100 mM NaCl		63.3	236
0.1 g/l/0.1–0.3 mM NaCl, 0.1 mM $CaCl_2$		63.3	419
Talc	$6.2{\cdot}10^{-9}$		
0.1 g/l/ 10 mM NaCl		67.5	112
Wood resin droplets	$1.4–2.7{\cdot}10^{-8}$ [1]		
0.1 g/l/ 10 mM NaCl	$2.42{\cdot}10^{-8}$	69.9	318.6
0.1 g/l/ 1 mM $CaCl_2$	2.10^{-8}	61.7	224

[1]From Kekkonen and Stenius [39].

Nevertheless, the differences observed between values calculated from Equations (1) and (5) are in most cases so large that they must be considered significant.

Adsorption of kaolin and polystyrene latex from the solutions with the lowest electrolyte concentrations (20 mM and 10 mM NaCl, respectively) is much slower than predicted by Equation (5). These concentrations are clearly close to the critical adsorption concentrations of electrolyte below which no adsorption is observed (1–1.5 mM NaCl for polystyrene latex and 10–11 mM NaCl for kaolin). Thus, the slow adsorption must be due to repulsion between electrical double layers on the surface and the adsorbates, which is still significant but obviously not large enough to prevent adsorption completely. Since the charge density of the polyurethane surface is not known, it is not possible to make a theoretical prediction of the actual repulsive interaction, but repulsion between negative surfaces in 10 or 20 mM NaCl is in the expected concentration range according to the DLVO theory.

The rate of polystyrene latex adsorption increases when double-layer repulsion is completely screened. Hence, the rate of adsorption of polystyrene latex becomes more or less completely controlled by diffusion in 100 mM NaCl and 0.1 mM $CaCl_2 + 0.1–0.3$ mM NaCl. The high adsorption calculated for these two solutions from QCM-D measurements is probably, to a large extent, due to overestimation by Equation (1).

For AKD, the amounts indicated by the application of Equation (1) for adsorption from 0.1 mM NaCl are so large that it seems likely that the adsorption of AKD is really faster than predicted for diffusion-controlled adsorption. This behaviour is expected, since the AKD particles have been rendered positive by adsorption of a polycation so that there is an attractive double-layer interaction driving the adsorption (heterocoagulation, bridging caused by the polymer that covers the particles). In accordance with this mechanism, the rate of adsorption decreases strongly when the salt concentration is increased to 10 mM (Table 7).

The adsorption of slowly coagulating wood resin droplets (10 mM NaCl and 1 mM $CaCl_2$) is mainly controlled by diffusion. The adsorption ceased in high salt concentrations, where the droplets were strongly coagulated (particle size 800–4000 nm during the adsorption). This is presumably due to their slower diffusion. The result is in harmony with the theory concerning rapidly and slowly coagulating dispersions [40]. The results are also in agreement with a previous study where the influence of salt conditions on the adsorption kinetics of wood resin droplets was investigated [41].

TABLE 8 Blocking Times (τ_{bl}) Interpreted from Results and Used in Fittings

Adsorbed substance and salt condition	Blocking time (min)
Kaolin in 20 mM NaCl	170
Polystyrene latex in 10 mM NaCl	580
Wood resin droplets in 10 mM NaCl	3.4

To account for the influence of already-adsorbed particles, we used the model suggested by Boluk and Van de Ven [42]. The rate of adsorption of colloids is given by

$$\Gamma = \left(\frac{d\Gamma}{dt}\right)_0 \tau_{bl}(1 - e^{-t/\tau_{bl}}), \tag{6}$$

where Γ is the amount adsorbed, $(d\Gamma/dt)_0$ is the initial rate of deposition, τ_{bl} is the blocking time, and t is the time from the beginning of the experiment. As a measure of the initial rate of deposition, we used $\Delta f/\Delta t$ after 1 min from the beginning of the adsorption. The characteristic blocking time is given by

$$\Gamma_{final} = \left(\frac{d\Gamma}{dt}\right)_0 \tau_{bl}. \tag{7}$$

Equations (6) and (7) were applied to cases in which, (1) the amount adsorbed was relatively low and depletion had only a moderate influence on adsorption, (2) it could be assumed that adsorbed particles did not spread on the surface and blocking effects remain unchanged during the adsorption, and (3) the $\Delta D/\Delta f$ plots did not radically change during adsorption (as with talc). When the requirements were fulfilled, a satisfactory fit could be made of experimental data to Equation (6). This was the case for the adsorption of wood resin droplets in 10 mM NaCl, polystyrene latex in 10 mM NaCl, and kaolin in 20 mM NaCl. Calculated blocking times (τ_{bl}) from these experiments are listed on Table 8, and an example of an adsorption curve fitted to Equation (6) is presented in Figure 22. In all three cases, the emptying of the chamber caused a small difference between the experimental (bold line) and theoretical (thin line) curves as seen in the middle part of the Figure 22.

Adsorption as Predicted DLVO theory

Adsorption of particles on the tested polyurethane materials behaved roughly, as predicted by diffusion-controlled adsorption with

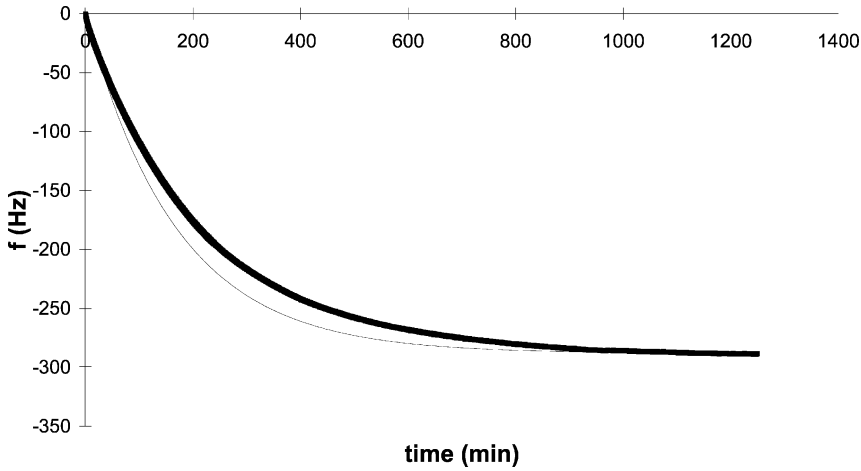

FIGURE 22 Observed (bold line) and theoretical (thin line) curves for the adsorption of kaolin in 20 mM NaCl and pH 7.

interaction energies predicted by DLVO theory. Several observations support this idea: (1), the surface charge determined the adsorption behaviour when the salt concentration was low. Positively charged substances adsorbed rapidly, but negatively charged ones did not adsorb or the adsorption was slow. (2), The influence of surface charge became smaller when the concentration of monovalent ions (Na^+, Cl^-) increased over 100 mM. At 300–500 mM NaCl, the effect of surface charge was negligible. (3), Divalent ions (SO_4^{2-}, Ca^{2+}) enhanced or prevented adsorption at much lower concentrations than monovalent ions (Na^+, Cl^-). SO_4^{2-} prevented the adsorption of cationic starch already in 100 mmol/l, while 300 mmol/l Cl^- was needed to do the same. Adsorption of PS-latex started when the concentration of Ca^{2+} exceeded 0.1–0.4 mmol/l or 1–1.5 mmol/l /l Na^+. In addition, critical salt concentrations, above which adsorption started to occur, were observed for negatively charged kaolin and polystyrene latex (1–1.5 mM NaCl for polystyrene latex, 10–12 mM NaCl for kaolin).

It was not necessary to invoke any surface forces other than those involved in the DLVO theory to explain the behaviour of polyurethane as adsorbent. Polyurethane, with a water contact angle of 60–70°, can be estimated to be too hydrophobic to cause any solvation forces and too hydrophilic to cause long-range hydrophobic attraction. No indications of steric interactions were observed, except the retardation of further adsorption by already-adsorbed particles. Earlier it has been

found that oxide surfaces occurring in paper machines also behave as predicted by DLVO theory [4, 27].

The Three-stage Model

With reference to the three-step model described in the Introduction, the following can be said. While the results strongly validate the importance of step 1, there was less evidence of the influence of step 2. For example, polystyrene latex particles adsorbed on polyamide and were easily moved by the AFM needle, presumably due to a small contact area and low adhesion of the particles. Thus, mechanical and hydrodynamic forces will probably easily detach latex particles. AKD wax (Figures 6 and 21) apparently had a large contact area and large adhesion on the surface after drying and possibly also in the wet state. It is, therefore, reasonable to assume that AKD deposits are difficult to remove from the polyurethane surface. The $\Delta D/\Delta f$ values of cationic starch indicate that viscoelasticity and adhesion of the deposits can be dependent on salt conditions.

With reference to step 3, experiments with sequential adsorption (Figure 12–19) showed that different kinds of adsorbed layers might easily collect further deposits (step 3). Indeed, adsorbed deposits were in some cases a requirement for the start of adsorption of some substances. At low salt concentration (0.1 mM NaCl) polystyrene latex did not adsorb on polyurethane. When positively charged AKD-wax was first adsorbed, latex particles started to adsorb (Figure 12). The same behaviour was observed with AKD and kaolin (Figure 13). No cases where the adsorbed layer would have prevented further adsorption were found. However, there are such observations in the literature. For example, a layer of dissolved and colloidal substances on an oxide surface prevents the adsorption of wood resin droplets [39].

Applications in Paper Making

Model deposits were easily brought in contact with surfaces by adsorption, which was sensitive to pH and salt concentrations. This observation is in harmony with the experiences from paper mills, where the changes in pH and salt conditions often cause fouling. Results indicate that if the surface and the fouling substance are similarly charged, the rise in salt concentrations over a critical limit may lead to adsorption of a first layer of fouling material. The adsorption of kaolin and PS-latex are examples of the influence of critical limits. Therefore, with respect to changes in salt conditions, the onset of fouling may often not be a gradual but instead a stepwise process.

The first layer of deposits is formed more rapidly at low salt conditions if the surface and the fouling substances are oppositely charged (*e.g.*, the adsorption of cationic starch and AKD). Indeed, to avoid the initiation of fouling, it is advisable to strive to keep polymer surfaces and the fouling substances similarly charged in paper mills operating at moderate salt concentrations. This recommendation is not valid in mills operating at high salt concentrations (more than 200–300 mmol/l of monovalent ions such as Na^+ and Cl^- or more than 10–20 mmol/l of divalent ions (Ca^{2+}, $SO_4{}^{2-}$)), where the influence of surface charge is significantly reduced.

The results indicate that fouling in a paper machine is, to a large extent, diffusion controlled. Hence, dissolved and colloidal substances may foul more than larger particles (aggregates) in stagnant point conditions. Adsorption (fouling) ceases due to decreases in adsorbate concentrations and due to blocking by already-adsorbed particles.

The AFM images indicated that the adsorbed substances covered the surface in two ways. Cationic starch formed an even, fully covering layer with an estimated thickness of the adsorbed layer of 15–20 nm. This implies that surface forces of the original surface will be strongly weakened and the surface chemistry of the fouling layer will mainly depend on the cationic starch. Particles, on the other hand, are adsorbed in a scattered fashion. The surface properties of the original surface will be of importance on areas where there are no adsorbed particles, so that both the original polyurethane surface and adsorbed particles control the fouling.

The viscoelastic properties of cationic starch depended significantly on salt conditions. Therefore, although starch viscosity/elasticity depends strongly on temperature, the effect of salt on fouling also must be taken into account.

Based on our results, it can also be estimated that in locations in a paper machine where there are no forces that continuously remove formed deposits, a nonfouled surface will exist only for a short time. Concentrations of substances used in experiments (0.1–0.5 g/l) were relatively high compared with the concentrations of fouling substances in process water. The adsorption was also rapid and the adsorbed amounts were relatively large. The situation is slightly different with polymer surfaces, which are used as felt or roll materials. They are typically intermittently in contact with the fouling process water for short times (tens or hundreds of milliseconds). After the contact the surfaces are showered and exposed to mechanical forces before a new contact with process water. This will clearly slow down fouling by weakly adhered substances (latex, clay, and talc) and perhaps also by hydrophobic substances (AKD) because the surfaces are kept

hydrophilic. Fouling substances also may lack time to adhere due to short contact time with the fouling process water.

REFERENCES

[1] Paulapuro, H., Wet Pressing, In: *Paper Making Part 1, Stock Preparation and Wet End*, Paulapuro, H., Ed., (Gummerus Printing, Jyväskylä, 2000), Chap. 8, pp. 285–340.

[2] Weise, U., Terho, J., and Paulapuro, H., Stock and water systems of the paper machine, In: *Paper Making Part 1, Stock Preparation and Wet End*, Paulapuro, H., Ed., (Gummerus Printing, Jyväskylä, 2000), Chap. 5, pp. 125–190.

[3] Kilpeläinen, R., Taipale, S., Marin, A., Kortelainen, P., and Metsäranta, S., Forming Fabrics, In: *Paper Making Part 1, Stock Preparation and Wet End*, Paulapuro, H., Ed. (Gummerus Printing, Jyväskylä, 2000), Chap. 7, pp. 253–284.

[4] Kekkonen, J., *Adsorption kinetics of Wood Materials on Oxides*, Doctoral thesis, Helsinki University of Technology, Helsinki, Finland, 2001.

[5] Blanco, A., Negro, C., Otero, D., Sundberg, K., Tijero, J., and Holmbom, B., *Nordic Pulp Paper Res. J*. **15**, 607–613 (2000).

[6] Fischer, B., *Wochenblatt Papierfabr.*, **127**, 895–900 (1999).

[7] Vappula, R., Tiilikka, J., and Slater, P., Press Fabrics, In: *Paper Making Part 1, Stock Preparation and Wet End*, Paulapuro, H., Ed. (Gummerus Printing, Jyväskylä, 2000), Chap. 9, pp. 342–381.

[8] Niskanen, J., Paper Machine Rolls, In: *Paper Making Part 1, Stock Preparation and Wet End*, Paulapuro, H., Ed. (Gummerus Printing, Jyväskylä, 2000), Chap. 10, pp. 383–430.

[9] Nylund, J., Lagus, O., and Eckerman, C., *Coll. Surf. A* **85**, 81–87 (1994).

[10] Van De Ven, T. G. M. and Mason, S. G., *Tappi J*. **64**, 171–175 (1981).

[11] Knubb, S. and Zetter, C., *Nordic Pulp Paper Res. J.*, **17**, 164–167 (2002).

[12] Plunkett, M. A., Dynamic Interactions of Interfacial Polymers, Ph.D. thesis, Department of Chemistry, Surface Chemistry, Royal Institute of Technology, Stockholm, 2002.

[13] Yaminsky, V., Ohnishi, S., and Ninham, B., Long-range hydrophobic forces due to capillary bridging, In: *Handbook of Surfaces and Interfaces of Materials* vol. 4, pp. 131–227 (2001).

[14] Höök, F., Rodahl, M., Brzezinski, P., and Kasemo, B., *Langmuir*, **14**, 729–734 (1998).

[15] Rodahl, M., Höök, F., and Kasemo, B., *Anal. Chem.*, **68**, 2219–2227 (1996).

[16] Höök, F., Development of a Novel QCM Technique for Protein Adsorption Studies, Doctoral Thesis, Chalmers University of Technology and Göteborg University, Gothenburg, 1997.

[17] Sauerbrey, G., *Arch Elektrotech. Übertragung* **18**, 617–624 (1964).

[18] Caruso, F. D., Furlong, N., and P. Kingshott, *J. Colloid Interface Sci.* **186**, 129–140 (1997).

[19] Yang, M. and Thompson, M., *Langmuir* **9**, 1990–1994 (1993).

[20] Urbakh, M. and Daikhin, L., *Langmuir* **10**, 2836–2841 (1994).

[21] Daikhin, L., Gileadi, E., Katz, G., Tsionsky, V., Urbakh, M., and Zagidulin, D., *Anal. Chem.* **74**, 554–561 (2002).

[22] Höök, F., Kasemo, B., Nylander, T., Fant, C., Sott, K., and Elwing, H., *Anal. Chem.* **73**, 5796–5804 (2001).

[23] Voinova, M. V., Rodahl, M., Jonson, M., and Kasemo, B., *Physica Scripta* **59**, 391–401 (1999).

[24] Hunter, R. J., *Zetapotential in Colloid Science* (Academic Press, New York, 1981), Chap. 3, pp. 59–124.
[25] Johansson, L.-S., *Microchim. Acta* **138**, 217–223 (2002).
[26] Tougaard, S. and Sigmund, P., *Phys. Rev. B* **25**, 4452–4466 (1982).
[27] Kekkonen, J., Laine, H., and Stenius, P., *TAPPI J.* **83**, 71 (2000).
[28] Kekkonen, J., Adhesional Properties of Polyamide 6 Fibers Used in Press Felts, Licentiatès Thesis, Helsinki University of Technology, Helsinki, Finland, 1996.
[29] Goodwin, J. W., Hearn, J., Ho, C. C., and Ottewill, R. H., *Colloid Polymer Sci.* **252**, 464–471 (1974).
[30] Swerin, A., Sjödin, U., and Ödberg, L., *Nord. Pulp Paper Res. J.* **8**, 389–398 (1993).
[31] Swerin, A., Ödberg, L., and Wågberg, L., *Nord. Pulp Paper Res. J.* **8**, 298–301 (1993).
[32] Sundberg, K., Pettersson, C., Eckerman, C., and Holmbom, B., *J. Pulp Paper Sci.* **22**, 248–252, (1996).
[33] Sundberg, K., Thornton, J., Holmbom, B., and Ekman, R. E., *J. Pulp Paper Sci.* **22**, 226–230, (1996).
[34] Kekkonen, J. and Stenius, P. *Colloids and Surf. A.* **156**, 357–372 (1999).
[35] Evans, D. F. and Wennerström, H., *The Colloidal Domain*, (VCH Publishers, Inc., USA, 1994), p. 215.
[36] Holmberg, M., Berg, J., Stemme, S., Ödberg, L., Rasmusson, J., and Claesson, P., "Surface force studies of Langmuir-Blodgett cellulose films," *J. Colloid Interface Sci.* **186**, 369–381 (1997).
[37] Bergström, L., *Adv. Coll. and Int. Sci.* **70**, 125–169 (1997).
[38] Crank, J., *The Mathematics of Diffusion* (Oxford University Press, London, 1956).
[39] Kekkonen, J. and Stenius, P., *Nord. Pulp Pap. Res. J.* **14**, 300–309 (1999).
[40] Van de Ven, T. G. M., *Colloidal Hydrodynamics* (Academic Press, London, 1989).
[41] Kekkonen, J. and Stenius, P., *Colloid Polym. Sci.* **116**, 57–66 (2000).
[42] Boluk, M. Y. and Van de Ven, T. G. M., *Colloids Surf.* **46**, 157–176 (1990).